



New insight into the ultra-long lifetime of excitons in organic–inorganic perovskite: Reverse intersystem crossing

Guanghao Meng^a, Yantao Shi^{a,*}, Xiangyuan Wang^a, Wei Wang^c, Shufeng Wang^c, Min Ji^a,
Ce Hao^{a,b,**}

^a State Key Laboratory of Fine Chemicals, Dalian University of Technology, Dalian 116024, Liaoning, China

^b State Key Laboratory of Fine Chemicals, Dalian University of Technology, Panjin 124221, Liaoning, China

^c State Key Laboratory for Artificial Microstructure and Mesoscopic Physics, Department of Physics, Peking University, Beijing 100871, China

ARTICLE INFO

Article history:

Received 28 June 2017

Revised 20 October 2017

Accepted 20 October 2017

Available online 6 November 2017

Keywords:

Inorganic–organic halide perovskite

Photophysics

Photoluminescence

Reverse intersystem crossing

Ultra-long lifetime

ABSTRACT

Recently, an effective exciton diffusion length L exceeding $100\ \mu\text{m}$ has been reported for organic–inorganic halide perovskites owing to both the high mobility and ultra-long lifetime of the excitons; however, the origin of ultra-long L is still unclear in nature. In some photoelectric materials, reverse intersystem crossing (RISC) from the triplet to the singlet state can enhance the quantum yield of photoluminescence greatly. In this study, our theoretical investigation indicated that the energy difference ΔE_{st} between the singlet state and the triplet state of $\text{CH}_3\text{NH}_3\text{PbI}_3$ was less than 0.1 eV, which represents one crucial prerequisite for the occurrence of RISC. Meanwhile, the experimental results showed that the photoluminescence lifetime increased with the increasing temperature, a typical feature of RISC. Based on this study, we put forward the hypothesis that the ultra-long lifetime of excitons in organic–inorganic halide perovskite might be caused by the RISC process. This may provide a new insight into the important photophysical properties of such novel photovoltaic materials.

© 2017 Science Press and Dalian Institute of Chemical Physics, Chinese Academy of Sciences. Published by Elsevier B.V. and Science Press. All rights reserved.

1. Introduction

As an emerging photovoltaic material, organic–inorganic halide perovskite has attracted considerable attention due to its desirable advantages, such as moderate band gap, facile solution processability, effective exciton dissociation, etc. [1–5]. Despite the high power conversion efficiency of over 20% that has been achieved for perovskite solar cells (PSCs) [6,7], some basic scientific enigmas of this fascinating material require further elaboration; for example, the ultra-long effective charge diffusion length L facilitates the exciton dissociation greatly [8,9]. In general, L is obtained with the following equation:

$$L = \sqrt{D\tau} \quad (1)$$

where τ is the exciton lifetime and D is the charge diffusion coefficient; these two important factors can be determined by transient absorption and photoluminescence-quenching measurements. It is evident that a large value of τ is one prerequisite for an ultra-long L , which has been confirmed experimentally [8,10]. In the mean-

time, researchers in this field are willing to determine the origin of these advantageous properties theoretically [11,12].

To date, there have been several explanations for the ultra-long τ of $\text{CH}_3\text{NH}_3\text{PbI}_3$. Based on optical investigations of a single crystal of $\text{CH}_3\text{NH}_3\text{PbI}_3$ from room temperature to 5 K, Fang et al. [13] attributed the ultra-long τ to the bound triplet exciton at temperatures below 160 K, while carriers recombination was induced by spontaneous radiative transitions from band to band at room temperature. On the other hand, Kong et al. [14] found that the longer τ of $\text{CH}_3\text{NH}_3\text{PbI}_3$ originated from free excitons and donor–acceptor-pair transitions. In brief, it can be seen that the early explanations on this issue are ambiguous. In some photoelectric materials, if the energy gap between the singlet and the triplet state is small enough, triplet excitons can return to the singlet state, which is called reverse intersystem crossing (RISC) [15,16]. This important photophysical process helps to increase the exciton's lifetime, which in turn achieves a higher quantum yield [15]. It is important to emphasize that perovskite materials have a periodic structure but to date, no method exists to calculate the excited state of the periodic structure accurately. Our group has proposed a method to deal with the excited state of materials with a periodic structure, such as MOFs [17–19]. To be specific, we selected representative structure units from MOFs by cutting off clusters based on their single crystal structures (obtained from experimental results); the

* Corresponding author.

** Corresponding author at: State Key Laboratory of Fine Chemicals, Dalian University of Technology, Dalian 116024, Liaoning, China.

E-mail addresses: shiyantao@dlut.edu.cn (Y. Shi), haoc@dlut.edu.cn (C. Hao).

clusters were calculated after saturation by hydrogen atoms at the boundary. So far, our method has been accepted as a valid strategy to deal with the excited state of periodic structures.

It is known that the singlet–triplet splitting energy (denoted as ΔE_{st} in our work) for inorganic semiconductors and organic molecules varies a lot. The ΔE_{st} of organic molecules has been reported to be 100–200 meV, much larger than that of inorganic materials [15]. $\text{CH}_3\text{NH}_3\text{PbI}_3$ is known as an organic–inorganic hybrid material with many amazing photoelectric properties. Inspired by these investigations, we firstly provided a new insight into the ultra-long τ of $\text{CH}_3\text{NH}_3\text{PbI}_3$ halide perovskite from the perspective of RISC. The experimental results showed that the photoluminescence lifetime increased with the increasing temperature [20,21], a typical feature of RISC. Meanwhile, the ΔE_{st} was then calculated to be 82 meV and 47 meV, which satisfies the prerequisite for the occurrence of RISC in thermally activated delayed fluorescence (TADF) photovoltaic materials [16,22,23]. It is conjectured that, for $\text{CH}_3\text{NH}_3\text{PbI}_3$, the semiconductor properties including ΔE_{st} are highly affected by the organic component. Based on this study, we put forward the hypothesis that the ultra-long lifetime of excitons in organic–inorganic halide perovskite might be caused by the RISC process. Our work provides a new insight into the important photophysical property of these novel photovoltaic materials.

2. Experimental

2.1. Experimental method

102.2 mg PbCl_2 and 174.9 mg $\text{CH}_3\text{NH}_3\text{I}$ were weighed. The materials were placed into a sample bottle, 0.5 mL *N,N*-dimethylformamide (DMF) was added and the mixture was heated at 70 °C for 1 h until mixed completely, followed by filtration. The solution and a glass substrate were transferred into a glove box and placed on a heating plate for preheating at 70 °C. After 70 μL of the solution was removed with a pipette, it was spin-coated on the substrate at 2000 rpm/30 s. First, it was heated at 90 °C for 1 h, then it was heated at 100 °C for 25 min, which completed the process for obtaining the $\text{CH}_3\text{NH}_3\text{PbI}_3$ film.

A streak camera (Hamamatsu C10910) was used to obtain the time-resolved photoluminescence (TRPL) spectra and the photoluminescence lifetime of the $\text{CH}_3\text{NH}_3\text{PbI}_3$ film from 80 K to 300 K.

2.2. Computational method

The structure of the $\text{CH}_3\text{NH}_3\text{PbI}_3$ cluster for ground state optimization was cut [24] from the crystal structure [25] of the tetragonal phases, as shown in Fig. 1. The lattice parameters a , b and c are equal to 8.8 Å, 8.8 Å, and 13.0 Å in the periodic tetragonal crystal structure. The lattice parameters α , β and γ are all equal to 90° in the periodic tetragonal crystal structure. According to the symmetry of the crystal structure, a lattice-site unit was cut from the tetragonal $\text{CH}_3\text{NH}_3\text{PbI}_3$ crystal structure to obtain a bigger cluster, namely one-fourth of the octahedral crystal structure. It has been suggested that the CH_3NH_3^+ cations in the tetragonal phase still occupy preferred orientations and a certain degree of long-range order [26]. The quantum chemical density functional theory (DFT) and time-dependent density functional theory (TD-DFT) were used to calculate the results using the Gaussian 09 software package [27]. All the atoms except the H atoms were frozen. The basis set Lanl2dz was used including the relativistic effect because Pb atom is heavy. The PBEPBE functional was used to calculate ΔE_{st} in conjunction with the MOMAP-v0.2.003 program developed by Shuai et al. [28–31] to calculate the rate of RISC of $\text{CH}_3\text{NH}_3\text{PbI}_3$. The parameter of the excited states was set to triplet only for the triplet state calculation, i.e., the electrons were excited to the triplet state.

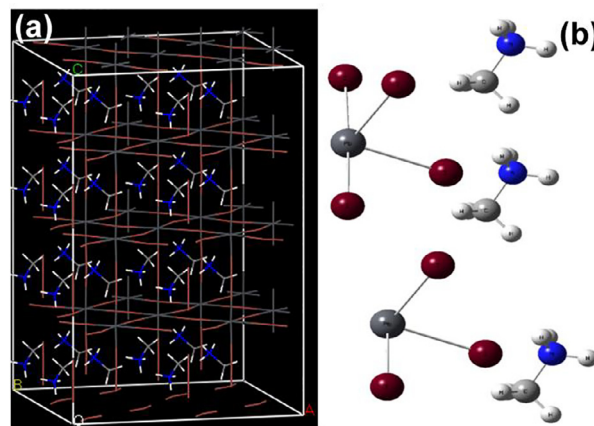


Fig. 1. (a) Tetragonal phases of $\text{CH}_3\text{NH}_3\text{PbI}_3$ crystal structure; (b) Calculative cluster model for ground state cut from the tetragonal crystal. The elements are represented by the following colors: N, blue; C, light gray; H, white; Pb, dark gray; and I, brown.

The peak position of the infrared (IR) spectrum and the maximal absorption in the ultraviolet–visible (UV–vis) spectrum of the $\text{CH}_3\text{NH}_3\text{PbI}_3$ cluster model were matched with the experimental results reported by Ahmed et al. [32] and Umari et al. [12], respectively, as shown in the Supporting Information.

Starting from the Fermi golden rule, as shown in Eq. (2), Shuai et al. derived the equations for calculating the rate of the photo-physical process [29,31], including the rate of fluorescence k_F , the rate of RISC k_{RISC} , the rate of internal conversion (IC) k_{IC} , and the rate of intersystem crossing (ISC) k_{ISC} . The i represents the initial state of $\text{CH}_3\text{NH}_3\text{PbI}_3$; f represents the final state; v represents the vibration in the initial state; v' represents the vibration in the final state; P is the Boltzmann distribution in Eq. (2). In Eq. (3), a and b are the vibration quantum numbers; c is the speed of light in a vacuum; Θ represents the vibration wave function; Q is the canonical coordinate of the nuclear motion; M_{if} is the transition dipole moment from the initial state i to the final state f , representing the electronic transition.

$$k = \frac{2\pi}{\hbar} \sum_{v,v'} P_{i,v} |H'_{iv,fv'}|^2 \delta(E_{f,v'} - E_{i,v}) \quad (2)$$

$$k_F = \frac{64\pi^4}{3hc^3} |M_{if}(0)|^2 \sum_a \sum_b v_{ib \rightarrow fa} \left| \int \Theta_{fa}(Q)^* \Theta_{ib}(Q) dQ \right|^2 \quad (3)$$

$$k_{\text{RISC}} = \frac{2\pi}{\hbar} \sum_v \sum_{v'} |\langle \phi_i \Theta_{i,v} | \hat{H}'_{\text{SO}} | \phi_f \Theta_{f,v'} \rangle|^2 \delta(E_{i,v} - E_{f,v'}) \quad (4)$$

$$k_{\text{IC}} = \frac{2\pi}{\hbar} \sum_{v,v'} P_{i,v} |\langle \phi_i \Theta_{f,v'} | \hat{H}'_{\text{BO}} | \phi_f \Theta_{i,v} \rangle|^2 \delta(E_{f,v'} - E_{i,v}) \quad (5)$$

$$k_{\text{ISC}} = \frac{2\pi}{\hbar} \sum_{v,v'} P_{i,v} |\langle \phi_f \Theta_{f,v'} | \hat{H}'_{\text{SO}} | \phi_i \Theta_{i,v} \rangle|^2 \delta(E_{f,v'} - E_{i,v}) \quad (6)$$

The rate of RISC is sensitive to temperature [33]. k_{RISC} increases at high temperature, as shown in Eq. (7).

$$k_{\text{RISC}} \propto \exp\left(\frac{\Delta E_{st}}{k_B T}\right) \quad (7)$$

3. Results and discussion

For the photoluminescence measurements, $\text{CH}_3\text{NH}_3\text{PbI}_3$ was prepared on a quartz glass by solution route. The structure diagram of the device is shown in Fig. 2(a). The X-ray diffraction

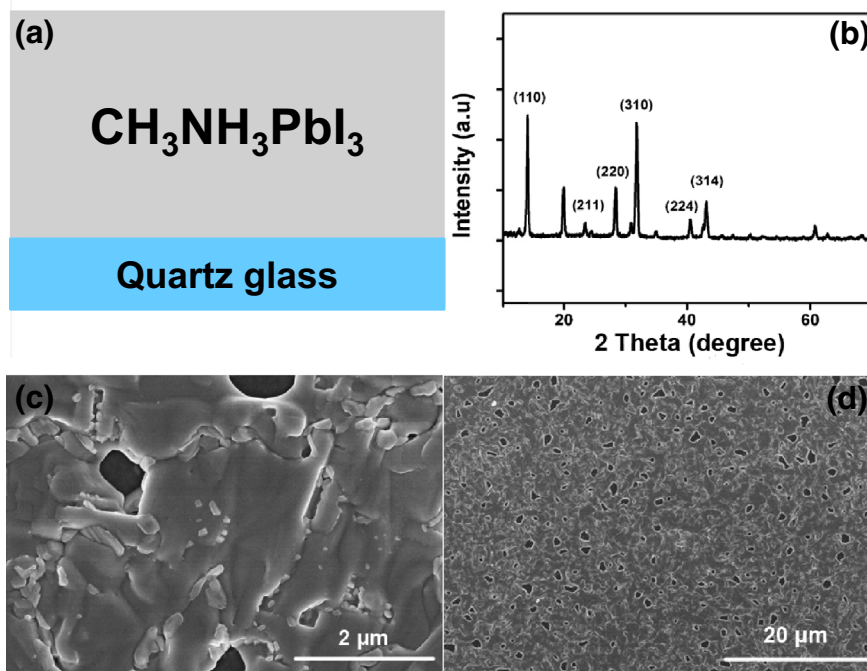


Fig. 2. (a) Schematic architecture of $\text{CH}_3\text{NH}_3\text{PbI}_3$ /Quartz glass; (b) XRD pattern of $\text{CH}_3\text{NH}_3\text{PbI}_3$; (c, d) Top-view SEM images of $\text{CH}_3\text{NH}_3\text{PbI}_3$.

(XRD) pattern in Fig. 2(b) indicates that the characterized diffraction peaks of the perovskite sample were well designated according to the standard JPSDS card, such as (1 1 0), (2 1 1), (2 2 0), and (3 1 0). The scanning electron microscopy (SEM) results (Fig. 2c and d) showed that the $\text{CH}_3\text{NH}_3\text{PbI}_3$ film was homogeneous and generated apparent holes.

Milot et al. [34] observed the two structural phase transitions occurring at 160 and 310 K. The monomolecular charge-carrier recombination rate increased with the rising temperature, indicating a mechanism dominated by ionized impurity mediated recombination. However, the lattice parameters of a tetragonal crystal are relatively similar to those of an orthorhombic crystal, which is thought to be not sufficient to influence their photophysical properties. It is well known that phosphorescence can be only observed at very low temperatures. Even if there is a phase transition in the $\text{CH}_3\text{NH}_3\text{PbI}_3$ perovskite, the RISC process may be still effective since ΔE_{st} between the singlet state and the triplet state of $\text{CH}_3\text{NH}_3\text{PbI}_3$ is less than 0.1 eV, which is a crucial prerequisite for the occurrence of RISC. As shown in the photoluminescence spectra of $\text{CH}_3\text{NH}_3\text{PbI}_3$ in Fig. 3(a), double peaks were observed at low temperatures in our experiment, e.g. at 80 K, 120 K and 140 K. Although some researchers [34] have stressed that such a double peak is closely related to the phase transition of $\text{CH}_3\text{NH}_3\text{PbI}_3$, here we still think that it could be caused by phosphorescence. Because the phase transition temperature of $\text{CH}_3\text{NH}_3\text{PbI}_3$ was observed to be 160 K, at which the orthorhombic phase changes into the tetragonal one. According to this study reported by Kong et al. [14], the orthorhombic phase could be well maintained between 13 K and 130 K. Thus, in our work, the appearance of double peak in this range can be inferred to be irrelevant to the phase transition. The energy difference between the maximum absorption peak of the fluorescence at 300 K and the phosphorescence at 80 K in the TRPL spectra is ΔE_{st} in the experiment based on Eq. (8). The photoluminescence lifetime of $\text{CH}_3\text{NH}_3\text{PbI}_3$ was tested at different temperatures, as shown in Fig. 3(b). The time period was 500 ns and the light intensity was 813 nJ cm^{-2} . The calculation method proposed by Wang et al. [35] was used to acquire the mean photo-generated lifetime of $\text{CH}_3\text{NH}_3\text{PbI}_3$ by Eq. (9), where A is a pre-

Table 1. Lifetime of photoluminescence decay under different temperatures.

| T (K) | 300 | 200 | 160 | 140 | 120 | 80 |
|-------------|-------|-------|------|------|-----|-----|
| τ (ns) | 299.3 | 108.2 | 58.4 | 12.3 | 9.9 | 6.7 |

exponential factor and τ is the lifetime. The TRPL measurements were fit to a two-exponential decay. It is worth mentioning that the lifetime increased as the temperature increased from 80 K to 300 K, as shown in Fig. 3(c) and Table 1. Herz [36] has reported that the trap-assisted recombination is a monomolecular process consisting of the capture of either a hole or an electron in the ionized impurity state. Auger recombination is a many-body process that consists of the recombination of a hole with an electron, as well as a momentum and energy transfer to either a hole or an electron, resulting in phonon absorption or emission. They both have a clear dependency on the temperature and electron traps have been identified as the dominant source of trap-assisted recombination in $\text{CH}_3\text{NH}_3\text{PbI}_3$ [37]. However, this is not contradictory to the RISC process in the $\text{CH}_3\text{NH}_3\text{PbI}_3$ system. The RISC process may be still effective since ΔE_{st} of $\text{CH}_3\text{NH}_3\text{PbI}_3$ is less than 0.1 eV and the photoluminescence lifetime increases with temperature. These are typical phenomena that correspond to the RISC process in photovoltaic materials [20,21].

$$\Delta E_{\text{st}} = \frac{1240}{754} - \frac{1240}{779} = 0.05 \text{ eV} \quad (8)$$

$$\langle \tau \rangle = \frac{A_1 \tau_1^2 + A_2 \tau_2^2}{A_1 \tau_1 + A_2 \tau_2} \quad (9)$$

Sun et al. [38] have calculated the energy difference between the singlet state S_1 and the triplet state T_1 for adiabatic ΔE_{st} energy of 17 photoelectric materials used in TADF-based organic light-emitting diode devices. The authors demonstrated the efficiency of a non-empirically tuned range-separated exchange functional in reproducing the experimentally lowest singlet excitation energies and the corresponding singlet–triplet gaps (derived from 0 to 0 transitions) described by Adachi et al. [39]. The calculation method we used is based on the work of Sun et al.

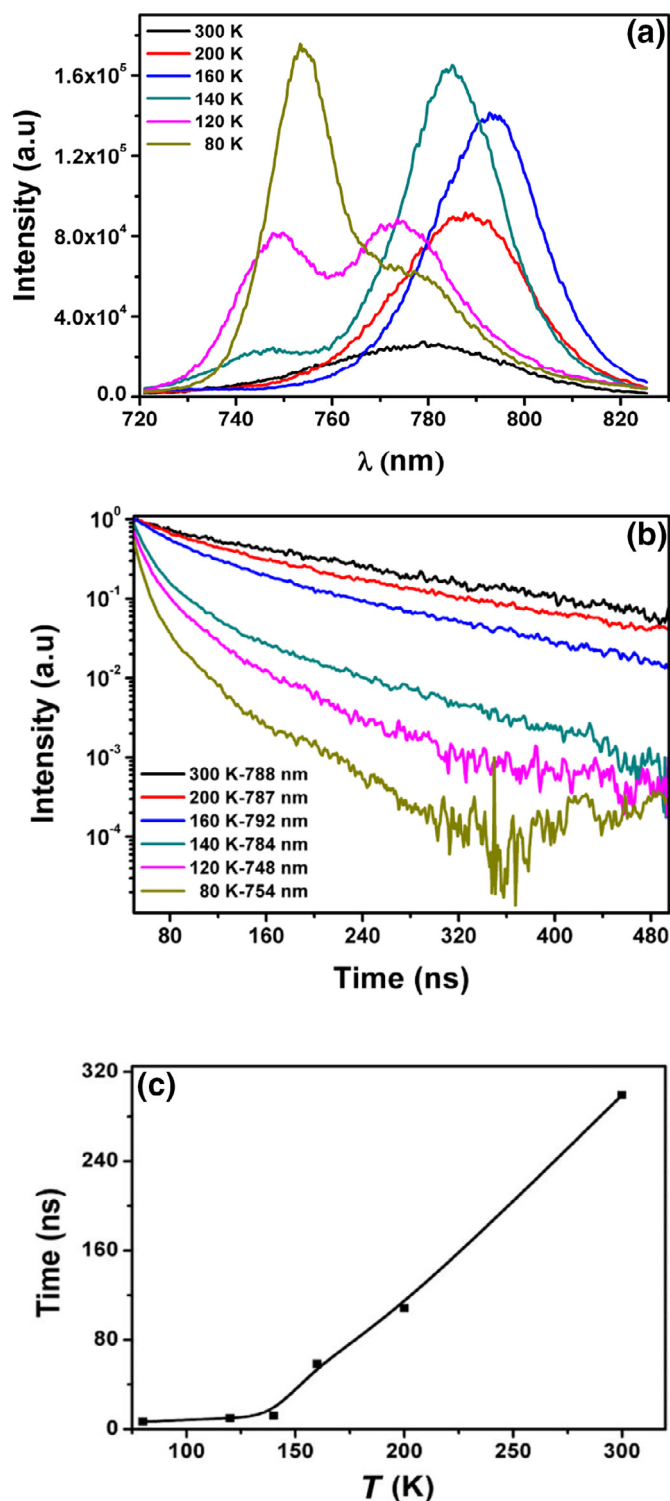


Fig. 3. Photoluminescence spectra (a) and lifetime (b) of $\text{CH}_3\text{NH}_3\text{PbI}_3$ at different temperatures; (c) Lifetime of photoluminescence decay as a function of temperature.

[38]. RISC occurs in photoelectric materials when the ΔE_{st} energy is less than 0.1 eV [40,41]. It is well known that the crystal phase of the $\text{CH}_3\text{NH}_3\text{PbI}_3$ perovskite varies with temperature; for example, the crystal phase is orthorhombic below 160 K and tetragonal in the range between 160 K and 327 K [42]. Our theoretical calculation results show that, for $\text{CH}_3\text{NH}_3\text{PbI}_3$ molecule, the adiabatic ΔE_{st} is 0.082 eV for the orthorhombic phase and 0.047 eV for the tetragonal

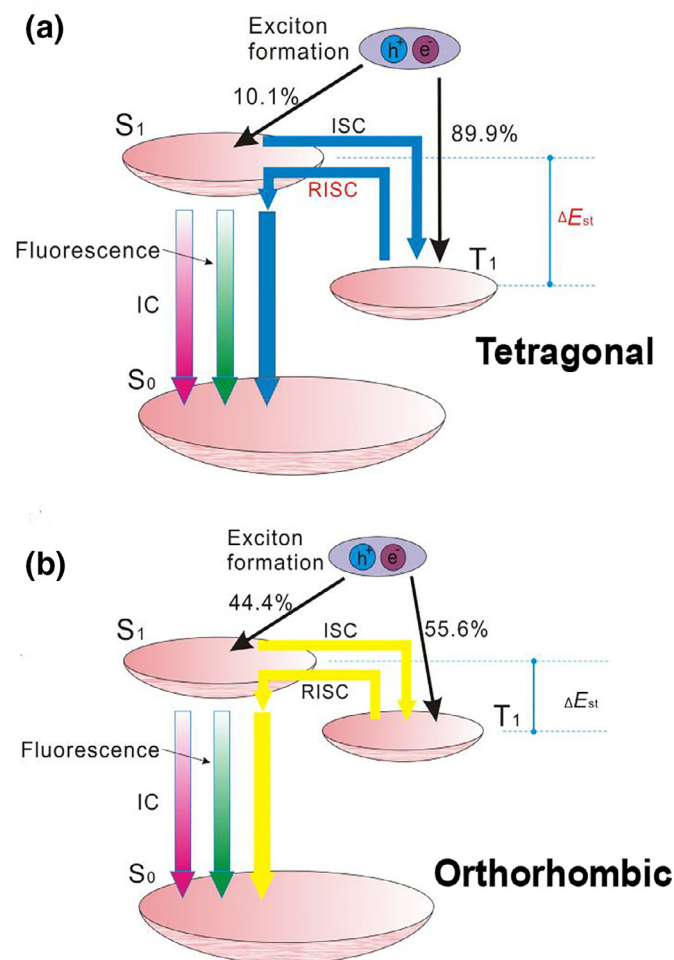


Fig. 4. RISC as a photophysical process in tetragonal (a) and orthorhombic (b) $\text{CH}_3\text{NH}_3\text{PbI}_3$.

onal phase. It is evident that RISC likely occurs in $\text{CH}_3\text{NH}_3\text{PbI}_3$ at room temperature at very small values of ΔE_{st} .

Indeed, the ΔE_{st} of inorganic semiconductors is usually caused by electron–hole exchange interaction and is relatively smaller (on the order of a few 10s meV) when compared to that of organic photoelectric materials (100–200 meV). $\text{CH}_3\text{NH}_3\text{PbI}_3$ is usually known as an organic–inorganic hybrid material. In our calculation, the model we pick up is based on a basic fragment rather than periodic structure. There is no energy band structure in the selected fragment, hence, the electronic states are more localized. In other words, the model we adopt for calculation has a strong quantum confinement effect if compared to a complete periodic system. From this point of view, the energy levels of single and triplet states as well as the ΔE_{st} (82 meV and 47 meV) calculated in our work could be larger the real values. Our present is expected to evoke special attention on this issue, but which still need further investigation either by optimizing computational methods or combining with well-designed experiments in future.

In $\text{CH}_3\text{NH}_3\text{PbI}_3$ perovskite, the singlet and triplet excitons formed after the electrons and holes were recombined. When ΔE_{st} was less than 0.1 eV, the triplet exciton returned to the S_1 state by thermal motion, namely the RISC process and harvested spin-forbidden T_1 excitons, as shown in Fig. 4. The rates of RISC in the tetragonal and orthorhombic $\text{CH}_3\text{NH}_3\text{PbI}_3$ molecules were $7.7 \times 10^8 \text{ s}^{-1}$ and $4.93 \times 10^9 \text{ s}^{-1}$, respectively, as shown in Table 2. The spin-forbidden transition from T_1 to S_0 was transferred into a singlet exciton by the RISC process, resulting in a significant in-

Table 2. Rates of photophysical processes in tetragonal and orthorhombic $\text{CH}_3\text{NH}_3\text{PbI}_3$.

| Crystal phase | $k_{\text{RISC}} (\text{s}^{-1})$ | $k_{\text{ISC}} (\text{s}^{-1})$ | $k_{\text{F}} (\text{s}^{-1})$ | $k_{\text{IC}} (\text{s}^{-1})$ |
|--------------------|-----------------------------------|----------------------------------|--------------------------------|---------------------------------|
| Tetragonal phase | 7.7×10^8 | 6.84×10^9 | 1.07×10^{12} | 3.12×10^{13} |
| Orthorhombic phase | 4.93×10^9 | 3.93×10^9 | 1.02×10^{13} | 4.45×10^{13} |

crease in the lifetime of the singlet exciton, which in turn leads to an ultra-long lifetime of the exciton in the $\text{CH}_3\text{NH}_3\text{PbI}_3$ perovskite. The rate of ISC in the tetragonal $\text{CH}_3\text{NH}_3\text{PbI}_3$ was $6.84 \times 10^9 \text{ s}^{-1}$, which was larger than the value of RISC. In contrast, the rate of ISC in the orthorhombic $\text{CH}_3\text{NH}_3\text{PbI}_3$ was $3.93 \times 10^9 \text{ s}^{-1}$, which was smaller than the value of RISC. The proportion of the singlet exciton to the triplet exciton was in equilibrium with the reverse concentration (Eq. (10)); thus, the proportion of the singlet exciton to the triplet exciton in the tetragonal phase of $\text{CH}_3\text{NH}_3\text{PbI}_3$ was 10.1%:89.9% and the proportion was 44.4%:55.6% in the orthorhombic $\text{CH}_3\text{NH}_3\text{PbI}_3$ phase. Quartz et al. [26] have reported that CH_3NH_3^+ cations in a tetragonal crystal structure generate strong bending in the valence and conduction bands, which could reduce the carrier recombination and delay the photoluminescence lifetime. In our calculation, k_{RISC} and k_{F} were both smaller in the tetragonal phase than in the orthorhombic phase, i.e., the lifetimes of RISC and the fluorescence were both longer in the tetragonal phase than in the orthorhombic phase. These results are in agreement with the report by Quartz et al.

$$\frac{k_{\text{te(ISC)}}}{k_{\text{te(RISC)}}} = \frac{k_{\text{te(S}_1)}}{k_{\text{te(T}_1)}} = \frac{c_{\text{te(T}_1)}}{c_{\text{te(S}_1)}} = \frac{89.9\%}{10.1\%} \quad (10)$$

4. Conclusions

With an increase in temperature, the photoluminescence lifetime of $\text{CH}_3\text{NH}_3\text{PbI}_3$ perovskite tended to increase; this phenomenon corresponds to the RISC process in the photovoltaic material. Furthermore, quantum chemical calculations showed that the adiabatic ΔE_{st} energy in the orthorhombic and tetragonal phases of $\text{CH}_3\text{NH}_3\text{PbI}_3$ perovskite was less than 0.1 eV. The rates of RISC in the tetragonal and the orthorhombic phases were $7.7 \times 10^8 \text{ s}^{-1}$ and $4.93 \times 10^9 \text{ s}^{-1}$, respectively, which further proved that the RISC process had occurred in the $\text{CH}_3\text{NH}_3\text{PbI}_3$ perovskite. Therefore, we put forward the hypothesis that the ultra-long lifetime of excitons in the $\text{CH}_3\text{NH}_3\text{PbI}_3$ organic–inorganic halide perovskite may be caused by the RISC process, which provides a new insight into the important photophysical properties of these novel photovoltaic materials.

Acknowledgments

The financial supports of the National Natural Science Foundation of China (grant nos. 21373042, 21677029 and 51402036), and the Fundamental Research Funds for the Central Universities (grant no. DUT15YQ109) are greatly appreciated.

References

- [1] G.E. Eperon, S.D. Stranks, C. Menelaou, M.B. Johnston, L.M. Herz, H.J. Snaith, *Energy Environ. Sci.* 7 (2014) 982–988.
- [2] J.H. Noh, S.H. Im, J.H. Heo, T.N. Mandal, S.I. Seok, *Nano Lett.* 13 (2013) 1764–1769.

- [3] H.S. Jung, N.G. Park, *Small* 11 (2015) 10–25.
- [4] H.S. Kim, C.R. Lee, J.H. Im, K.B. Lee, T. Moehl, A. Marchioro, S.J. Moon, R. Humphry-Baker, J.H. Yum, J.E. Moser, *Sci. Rep.* 2 (2012) 591–597.
- [5] Y. Shi, Y. Xing, Y. Li, Q. Dong, K. Wang, Y. Du, X. Bai, S. Wang, Z. Chen, T. Ma, *J. Phys. Chem. C* 119 (2015) 15868–15873.
- [6] N.J. Jeon, J.H. Noh, W.S. Yang, Y.C. Kim, S. Ryu, J. Seo, S.I. Seok, *Nature* 517 (2015) 476–480.
- [7] D. Bi, W. Tress, M.I. Dar, P. Gao, J. Luo, C. Renevier, K. Schenk, A. Abate, F. Giordano, J.P.C. Baena, *Sci. Adv.* 2 (2016) e1501170–e1501177.
- [8] S.D. Stranks, G.E. Eperon, G. Grancini, C. Menelaou, M.J. Alcocer, T. Leijtens, L.M. Herz, A. Petrozza, H.J. Snaith, *Science* 342 (2013) 341–344.
- [9] G. Xing, N. Mathews, S. Sun, S.S. Lim, Y.M. Lam, M. Grätzel, S. Mhaisalkar, T.C. Sum, *Science* 342 (2013) 344–347.
- [10] Q. Dong, Y. Fang, Y. Shao, P. Mulligan, J. Qiu, L. Cao, J. Huang, *Science* 347 (2015) 967–970.
- [11] C. Bernal, K. Yang, *J. Phys. Chem. C* 118 (2014) 24383–24388.
- [12] P. Umari, E. Mosconi, F. De Angelis, *Sci. Rep.* 4 (2014) 4467–4474.
- [13] H.H. Fang, R. Raissa, M. Abdu-Aguye, S. Adjokatse, G.R. Blake, J. Even, M.A. Loi, *Adv. Funct. Mater.* 25 (2015) 2378–2385.
- [14] W. Kong, Z. Ye, Z. Qi, B. Zhang, M. Wang, A. Rahimi-Iman, H. Wu, *Phys. Chem. Chem. Phys.* 17 (2015) 16405–16411.
- [15] Y. Tao, K. Yuan, T. Chen, P. Xu, H. Li, R. Chen, C. Zheng, L. Zhang, W. Huang, *Adv. Mater.* 26 (2014) 7931–7958.
- [16] H. Zhang, Y. Shi, F. Yan, L. Wang, K. Wang, Y. Xing, Q. Dong, T. Ma, *Chem. Commun.* 50 (2014) 5020–5022.
- [17] M. Ji, X. Lan, Z. Han, C. Hao, J. Qiu, *Inorg. Chem.* 51 (2012) 12389–12394.
- [18] M. Ji, C. Hao, D. Wang, H. Li, J. Qiu, *Dalton Trans.* 42 (2013) 3464–3470.
- [19] X. Sui, M. Ji, X. Lan, W. Mi, C. Hao, J. Qiu, *Inorg. Chem.* 52 (2013) 5742–5748.
- [20] S.Y. Lee, T. Yasuda, Y.S. Yang, Q. Zhang, C. Adachi, *Angew. Chem.* 126 (2014) 6520–6524.
- [21] S. Wang, X. Yan, Z. Cheng, H. Zhang, Y. Liu, Y. Wang, *Angew. Chem. Int. Ed.* 54 (2015) 13068–13072.
- [22] Q. Zhang, B. Li, S. Huang, H. Nomura, H. Tanaka, C. Adachi, *Nat. Photonics* 8 (2014) 326–332.
- [23] H. Uoyama, K. Goushi, K. Shizu, H. Nomura, C. Adachi, *Nature* 492 (2012) 234–238.
- [24] X. Dong, X. Fang, M. Lv, B. Lin, S. Zhang, J. Ding, N. Yuan, *J. Mater. Chem. A* 3 (2015) 5360–5367.
- [25] J. Feng, B. Xiao, *J. Phys. Chem. Lett.* 5 (2014) 1278–1282.
- [26] C. Quarti, E. Mosconi, F. De Angelis, *Chem. Mater.* 26 (2014) 6557–6569.
- [27] M.J. Frisch, G.W. Trucks, H.B. Schlegel, G.E. Scuseria, M.A. Robb, J.R. Cheeseman, G. Scalmani, V. Barone, B. Mennucci, G.A. Petersson, H. Nakatsuji, M. Caricato, X. Li, H.P. Hratchian, A.F. Izmaylov, J. Bloino, G. Zheng, J.L. Sonnenberg, M. Hada, M. Ehara, K. Toyota, R. Fukuda, J. Hasegawa, M. Ishida, T. Nakajima, Y. Honda, O. Kitao, H. Nakai, T. Vreven, J.A. Montgomery, Jr., J.E. Peralta, F. Ogliaro, M. Bearpark, J.J. Heyd, E. Brothers, K.N. Kudin, V.N. Staroverov, T. Keith, R. Kobayashi, J. Normand, K. Raghavachari, A. Rendell, J.C. Burant, S.S. Iyengar, J. Tomasi, M. Cossi, N. Rega, J.M. Millam, M. Klene, J.E. Knox, J.B. Cross, V. Bakken, C. Adamo, J. Jaramillo, R. Gomperts, R.E. Stratmann, O. Yazyev, A.J. Austin, R. Cammi, C. Pomelli, J.W. Ochterski, R.L. Martin, K. Morokuma, V.G. Zakrzewski, G.A. Voth, P. Salvador, J.J. Dannenberg, S. Dapprich, A.D. Daniels, O. Farkas, J.B. Foresman, J.V. Ortiz, J. Cioslowski, D.J. Fox, Gaussian, Inc., Wallingford CT, 2010.
- [28] Q. Peng, Y. Yi, Z. Shuai, J. Shao, *J. Chem. Phys.* 126 (2007) 114302–114310.
- [29] Q. Peng, Y. Yi, Z. Shuai, J. Shao, *J. Am. Chem. Soc.* 129 (2007) 9333–9339.
- [30] Y. Niu, Q. Peng, Z. Shuai, *Sci. China Ser. B: Chem.* 51 (2008) 1153–1158.
- [31] Y. Niu, Q. Peng, C. Deng, X. Gao, Z. Shuai, *J. Phys. Chem. A* 114 (2010) 7817–7831.
- [32] T. Ahmed, T. Salim, Y. Lam, E.E. Chia, J.X. Zhu, *EPL (Europhys. Lett.)* 108 (2015) 67015–67021.
- [33] Y. Suzuki, Q. Zhang, C. Adachi, *J. Mater. Chem. C* 3 (2015) 1700–1706.
- [34] R.L. Milot, G.E. Eperon, H.J. Snaith, M.B. Johnston, L.M. Herz, *Adv. Funct. Mater.* 25 (2015) 6218–6227.
- [35] X. Wang, X. Liu, C.-J. Tong, X. Yuan, W. Dong, T. Lin, L.M. Liu, F. Huang, *J. Mater. Chem. A* 4 (2016) 7762–7771.
- [36] L.M. Herz, *Annu. Rev. Phys. Chem.* 67 (2016) 65–89.
- [37] X. Fu, D.A. Jacobs, F.J. Beck, H. Shen, K.R. Catchpole, T.P. White, *Phys. Chem. Chem. Phys.* 18 (2016) 22557–22564.
- [38] H. Sun, C. Zhong, J.L. Brédas, *J. Chem. Theory Comput.* 11 (2015) 3851–3858.
- [39] S. Huang, Q. Zhang, Y. Shiota, T. Nakagawa, K. Kuwabara, K. Yoshizawa, C. Adachi, *J. Chem. Theory Comput.* 9 (2013) 3872–3877.
- [40] H. Nakanotani, T. Higuchi, T. Furukawa, K. Masui, K. Morimoto, M. Numata, H. Tanaka, Y. Sagara, T. Yasuda, C. Adachi, *Nat. Commun.* 5 (2014) 4016–4023.
- [41] S. Hirata, Y. Sakai, K. Masui, H. Tanaka, S.Y. Lee, H. Nomura, N. Nakamura, M. Yasumatsu, H. Nakanotani, Q. Zhang, K. Shizu, H. Miyazaki, C. Adachi, *Nat. Mater.* 14 (2015) 330–336.
- [42] E. Mosconi, C. Quarti, T. Ivanovska, G. Ruani, F. De Angelis, *Phys. Chem. Chem. Phys.* 16 (2014) 16137–16144.